TURBOMACHINERY & PUMP SYMPOSIA | VIRTUAL
DECEMBER 8-10, 2020
SHORT COURSES: DECEMBER 7, 2020

PERFORMANCE OF ADDITIVE MANUFACTURED HYDRODYNAMIC TILTING PAD BEARINGS WITH INTERNAL PAD COOLING

Dirk Schoenwald
Core Technology, Rotordynamics
Siemens Energy, Gas and Power
Duisburg, Germany

Axel Spanel
Product Design, Head of Integrally Gear Type Compressors
Siemens Energy, Gas and Power
Duisburg, Germany

Christoph Hoehnerbach
Manufacturing, Head of Technology and Programming
Siemens Energy, Gas and Power
Duisburg, Germany

Martin Biesenbach
Core Technology, Materials and Welding
Siemens Energy, Gas and Power
Duisburg, Germany

Dirk Schoenwald is a development engineer in the Core Technology Rotordynamics group at Siemens Energy's Gas and Power Division. In his more than 20 years with the company in Duisburg he has been working in the field of rotordynamics and bearings. His job profile includes theoretical and experimental work as well as providing calculation modules and design rules for design automation. He received a diploma degree (Dipl.-Ing.) in Mechanical Engineering from the University of Duisburg-Essen, Germany in 1999. Dirk Schoenwald is member of the VDI.

Axel Spanel heads the Frame Development of Gear Type Compressors at Siemens Energy's Gas and Power Division in Duisburg. He has been employed in Duisburg since obtaining his degree (Dipl.-Ing.) in mechanical engineering from the University of Applied Sciences "Niederrhein" in Krefeld, Germany (1991). His job functions include design standardization by providing a building block system with rules for process automation. Axel Spanel is member of the VDI and holds 2 patents.

Christoph Hoehnerbach is a Mechanical Engineer at Siemens Energy's Gas and Power Division in Duisburg, Germany. He joined Siemens Energy in 2007 and has since been involved in technology development in the manufacturing environment. His responsibilities also include machine investment decisions. Mr. Hoehnerbach graduated in Mechanical Engineering as an engineer in 1987 at the RWTH Aachen University, Germany.

Martin Biesenbach is a Materials Engineer at Siemens Energy's Gas and Power Division in Duisburg, Germany. He joined Siemens Energy in 2000 and has since been involved in materials related R&D projects, production and aftermarket support. He also has experience in the area of welding and brazing, thermal spraying and protective coatings. Dr. Biesenbach graduated in materials science as an engineer (1993) and received his Ph.D. degree in 2001 from the RWTH Aachen University, Germany. He is a member of DVS - German Welding Society.

ABSTRACT

The demand for higher power densities in gear-type compressors is pushing the loading of its already highly loaded pinions to even higher levels. The typically applied tilting-pad bearings are exposed to high circumferential speeds and high specific bearing loads, thus causing high bearing pad temperatures. The bearing design and especially the maximum realizable pad temperature becomes more and more the limiting design factor. With the draft of the next API 617 9th Edition, tightening the maximum acceptable bearing pad temperature to 203°F (95°C), bearing performance will become an even more determining factor for sound turbomachinery performance.

This paper presents a bearing pad design with three-dimensional cooling ducts inside the pad, realized by means of additive manufacturing (AM). A full-scale bearing test-rig was applied for extensive bearing testing up to circumferential speeds of 459.3 ft/s (140m/s) and specific bearing loads up to 362.6 PSI (25bar). Comparisons of the test results with conventionally manufactured bearing pads show the potential of AM bearing pads not only for gear-type compressors but also for high speed and low load turbomachinery.

INTRODUCTION

Gear-type compressors as shown in Figure 1 enable different compression services or inter-stage cooling in one turbomachine. Their inherent use of driving several pinions with two impellers each via a central bull gear allows for running the compressor stages in their optimum operating speed, thus realizing high volume flows and good energy efficiencies even under part load.

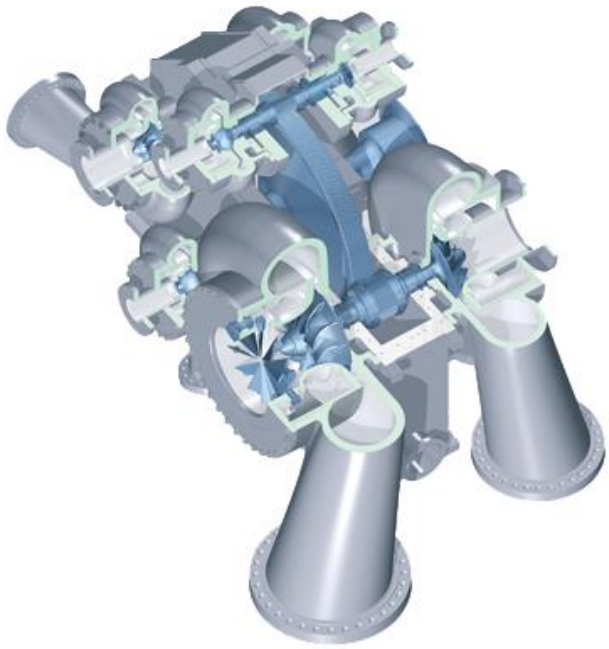

Figure 1. Illustration of a Gear-Type Compressor

Providing several advantages, the gear also comes along with some drawbacks. The windage losses of bull gears and pinions contribute to the overall power losses of a gear-type compressor. The bearing loads are mainly driven by the gear mesh forces in some instances greatly exceeding the weight load of the pinions. Foot-print reduction and increasing power density are means to increase competitiveness, thus causing even higher bearing loads. Increased oil flows and/or switching to copper-chrome as bearing base material are common practice to lower the maximum bearing pad temperatures and to comply with API 617 (2014) requirements. Several authors (Brockwell et al. 1992, Hirotoshi 2015, Livermore-Hardy and Blair 2014, Minegishi and Taketomi 2014, Nicholas et al. 2014) tried to optimize the oil supply to the bearing pads or to optimize the heat transfer from the bearing pads to the lubricating oil by increasing the pads' surface or by using special oil guiding components between the pads (Nicholas 2003). This paper describes an internal pad cooling approach for bearing cooling. Three dimensional channels inside the bearing pads are used to provide adequate cooling to the pads and to allow for higher specific bearing loads and high circumferential speeds. What is different from the approaches up to now is the manufacturing method of the cooled pads. Whereas the former approaches (Sato et al 2016, Becker 2000, Takeshi et al 2009) proposed conventional production methods to manufacture the cooling channels, the described approach uses additive manufacturing methods to fabricate one single pad with internal channels. A full-scale bearing test rig available at the authors' facility was used to perform comprehensive bearing testing with varying circumferential speed, specific bearing load and oil supply flow. The measured temperature profiles are compared with data captured on the same test-rig for a conventionally manufactured bearing.

BASELINE BEARING DESIGN

The bearing used for this study is a five-pad tilting pad bearing of rocker-back pivot style with 4.33 in (110 mm) diameter, a length to diameter ratio (L/D) of 0.7, a radial bearing clearance of 0.00559 in (0.142 mm, 2.58 ‰ relative bearing clearance) and a preload of 0.254 as shown in Figure 2. Its design results from an internal research project of the authors' company two decades ago. It was designed to allow for specific bearing loads up to 348.1 PSI (24 bar) and circumferential speeds up to 328.1 ft/s (100m/s) for use in gear-type compressors. The five pads are of different design. Two (large) pads with arc angles of 70+ degrees and offset pivot at the bottom carry the load whereas three (small) pads with smaller arc angles at the top serve mainly as guide pads only. A larger preload of the smaller top pads is intended to avoid pad flutter. Lubrication oil to the load carrying pads is directed through the pad support and guided internally to an inlet groove at the pad's leading edge to enter the lubrication gap. A pad integrated scraper at the trailing edge of the large pads removes the oil from the whirling shaft in order to reduce hot oil carryover to the next downstream pad. Figure 3 shows the load carrying (large) pads.

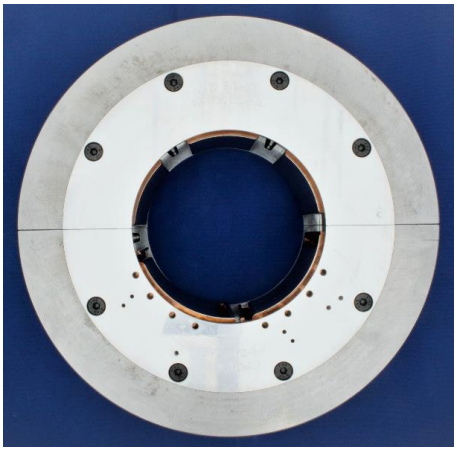

Figure 2. Tilting Pad Bearing Used for Testing

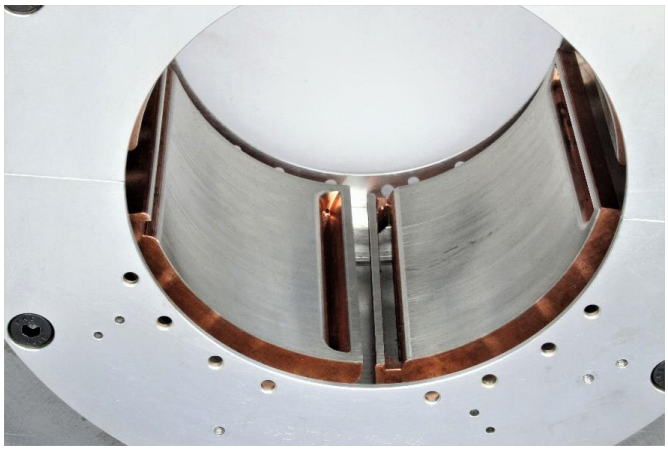

Figure 3. Load Carrying Pads

Lubricating oil to the small pads is provided by nozzles in front of each pad. The installation angle of the bearings is circumferentially adapted to the gear dependent load vector in order to realize a load between pivot situation. Copper-chrome as base pad material is used due to its high heat conduction capabilities. The bearing pads are manufactured conventionally, i.e. by milling, turning, drilling and centrifugal casting. Currently, there are more than 900 bearings of this type with different diameters and L/D ratios in operation.

ADDITIVE MANUFACTURING (AM) IMPROVEMENTS

In order to concentrate on the additional degrees of freedom available for the pad design, the geometrical properties of the printed load carrying pads with respect to pad arc angle, L/D ratio, preload, relative bearing clearance and pad support are unchanged. In addition, this approach allows for direct comparison of the effect of the internal cooling on pad temperatures. Focus was to generate a tilting pad with a large surface area in combination with a very stiff design. The AM bearing pad in Figure 4 is the result of a workshop held at the authors' facility together with third party AM experts.

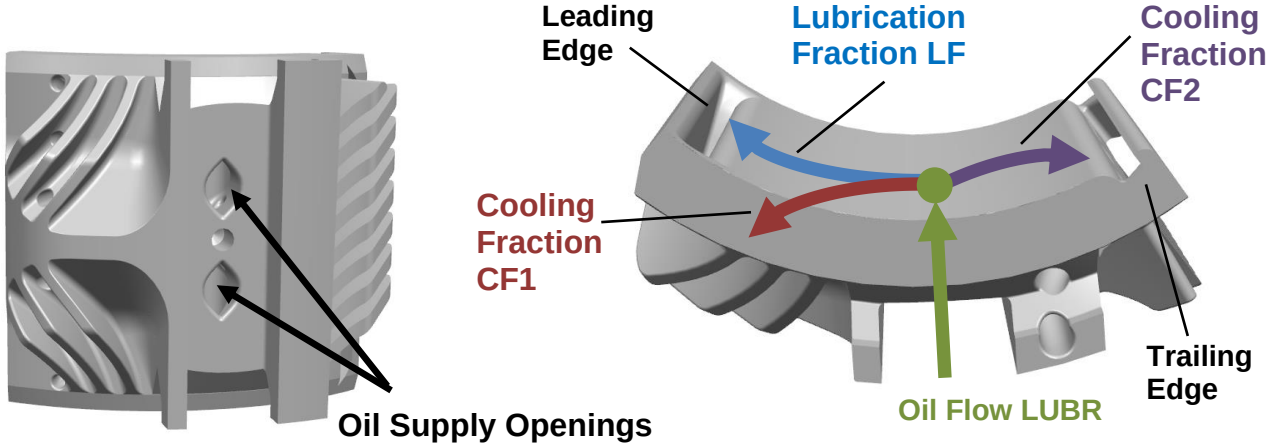

Figure 4. Outer Surface of AM Pad and Visualization of Pad Internal Oil Flow

Lubricant is supplied through the pad support by two openings to two plenum chambers, thus dividing the oil flow (LUBR) into three main flows; one for lubrication and two for cooling purpose. The lubrication part (LF) is directed to the leading edge of the pad to supply the amount of oil required for the hydrodynamic pressure generation. One of the cooling fractions (CF1) is directed to the leading edge of the pad where it leaves the pad at its backside between the heat exchanging fins. The other (CF2) is directed to the trailing edge of the pad to leave between pad and attached oil scraper.

The curved fins at the leading edge of the pad's backside are intended to direct the hot oil coming from the upstream pad to the outside in the axial direction. In addition, they are designed to stiffen the pad and minimize the radial deflection under high loading conditions. The large surface of the fins in combination with the cooling oil leaving the pad between the fins ensure a large heat transfer from the pad to the oil. Additional fins at the trailing edge of the pad's backside are also intended to generate high heat exchange. Thermocouple end positions are identical to the baseline pad. Due to the applied channels inside the pads, the thermocouple supplies are not straight channels, but three dimensional distorted. Pad sections with the thermocouple locations and their supplies have been printed in plastic material to check for the thermocouples' installation feasibility as depicted in Figure 5.

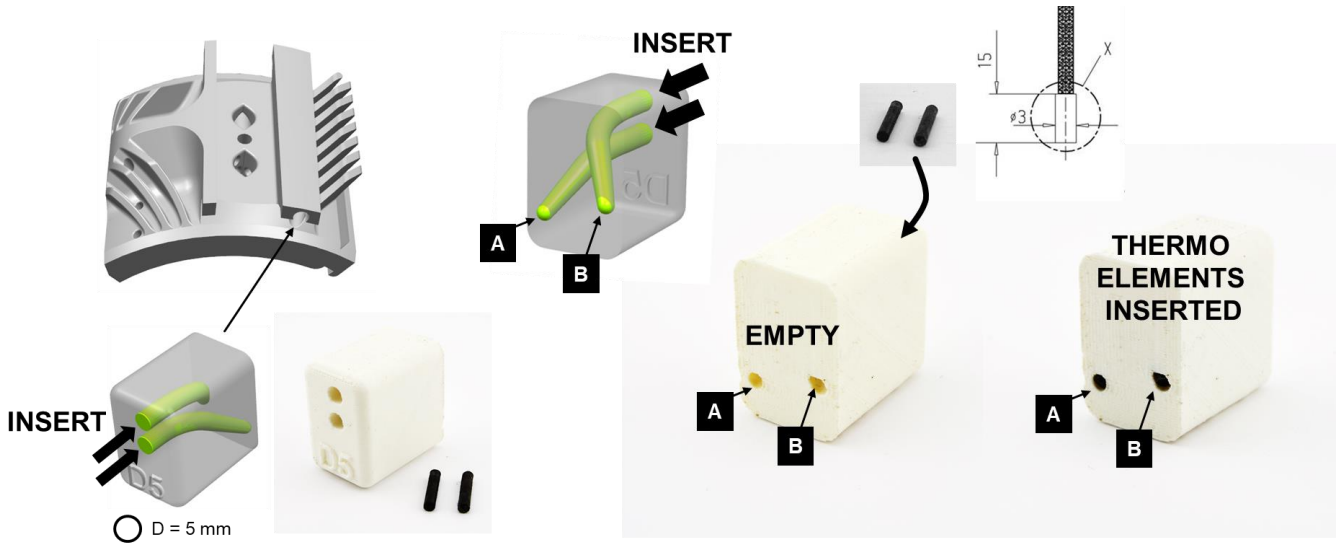

Figure 5. Installation Check for Thermocouples

MANUFACTURING

The AM pads were manufactured by Selective Laser Melting (SLM) sub-contracted to an AM-fabrication company. In order to make best use of the printer's manufacturing chamber, 4 pads were printed in one single setting accompanied by test specimen for material testing. After cutting the pads from the printer's base frame a heat treatment procedure was applied to the pads and to the test specimen in order to achieve the required material properties. Figure 6 shows the printed pads before white metal application and final machining.

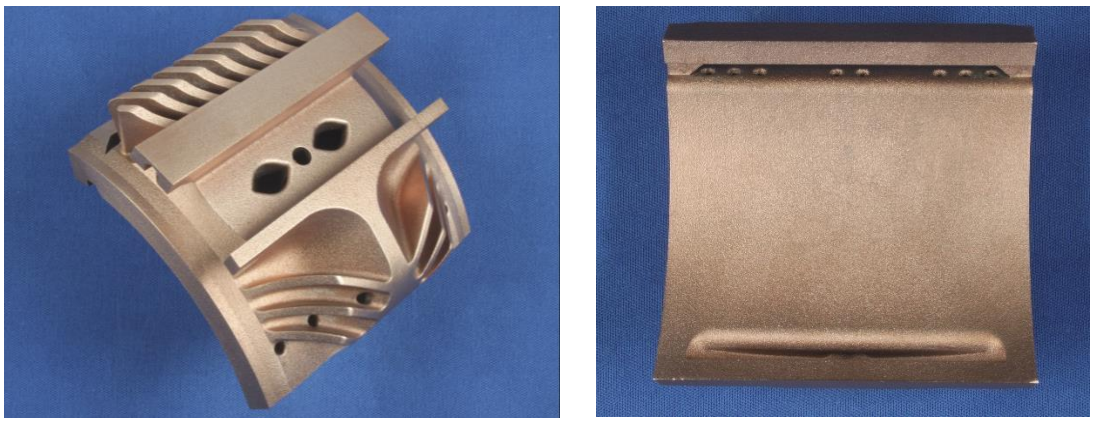

Figure 6. Printed Pads before White Metal Application and Final Machining

WHITE METAL COATING AND FINAL MACHINING

White metal coating of the printed pads was achieved by using arc spraying technology provided by an external supplier. The Babbitt material has the form of a wire and is fed to an arc spray gun. Applying voltage to the wire and the pad results in an electric arc, thus attaching the Babbitt material to the pad with a thickness of approximately 0.031 inches (800 µm). Figure 7 below shows a pad and a test specimen after arc spraying.
Extensive material testing such as bending tests, tensile adhesive strength testing, hardness testing and tensile strength testing of the pad base material and the coating proved to be in the magnitude of the materials' characteristics of forged CuCr base material and centrifugal casted Babbitt material.

Figure 7. Bearing Pad and Test Specimen after Arc Spraying

Final machining of the pads was done in the authors' facility. Inlet groove at the pad's leading edge and scraper window were opened with a side milling cutter. A mandrel was used to achieve the required preload dimensions. The relative bearing clearance was adjusted by grinding the corresponding shims of the pad supports.

TEST RIG

The full-scale test-rig as shown in Figure 8 used for testing the two different bearing pad designs consists of a drive unit and a variable test area accommodating the test specimen or test set-up according to the current research topic. The drive unit of this multi-purpose rotor test-rig comprises of a frequency converter driven electric motor and a planetary gear, thus allowing for maximum test speeds of 25477 rpm or 479 ft/s (146 m/s) sliding speed.

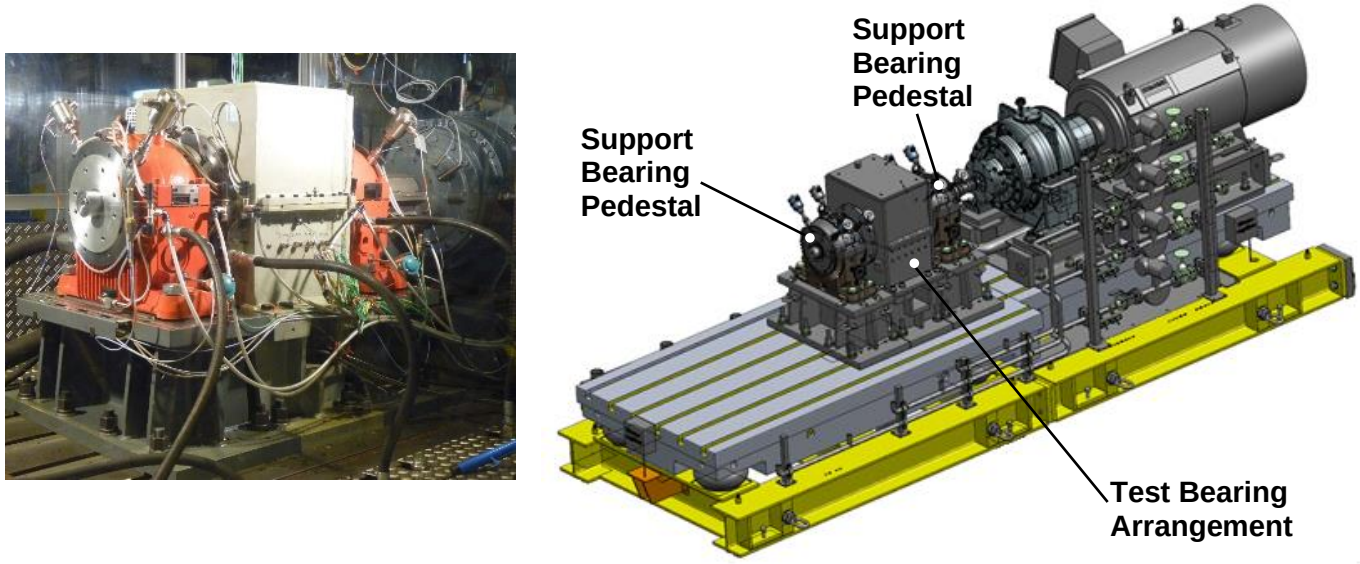

Figure 8. Multi-Purpose-Rotor-Test-Rig with Set-Up for Bearing Testing

Two tilting pad bearings of the described baseline design are implemented in separate bearing pedestals to support the test shaft and enclose the test bearing arranged between them. Figure 9 provides a cross section view of the detailed arrangement of the rig's test bearing section.

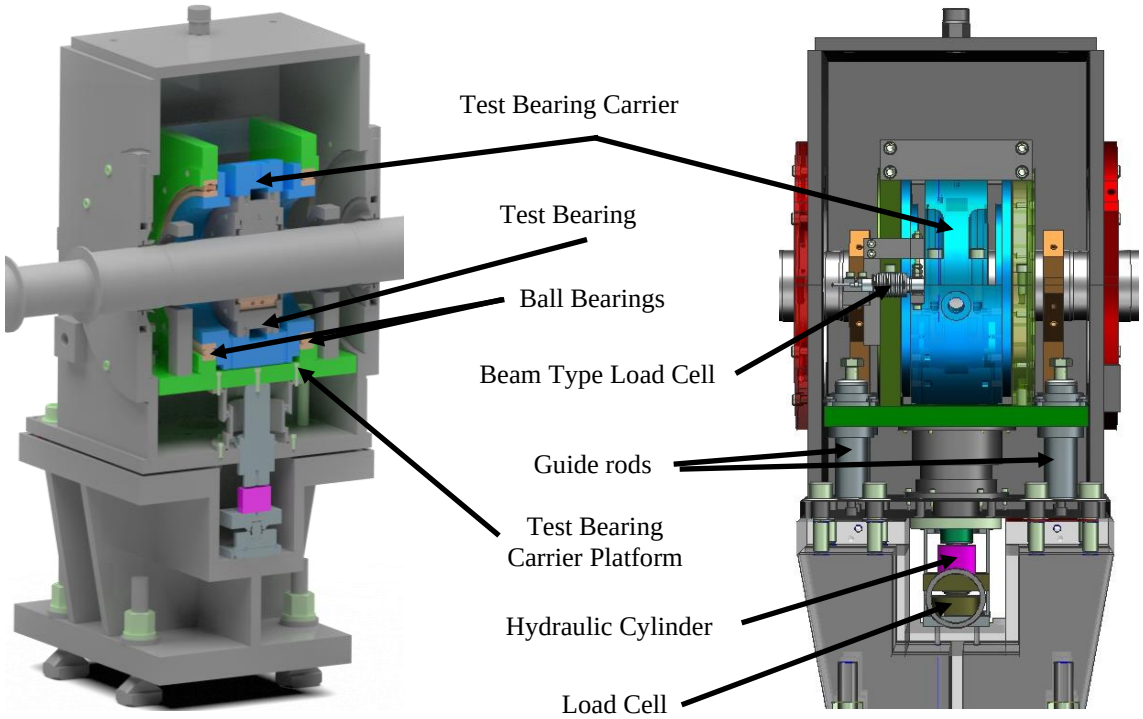

Figure 9. Cross Section of Detailed Test Arrangement

The test bearing is mounted to a test bearing carrier which itself is supported by two ball bearings, theoretically allowing the test bearing carrier to freely spin around the test shaft. A beam type load cell connected to the test bearing carrier and the stationary part of the ball bearing housing prohibits this movement and is used to determine the power loss of the test bearing. Four guide rods retain the test bearing carrier platform's axial position. A hydraulic cylinder struts against a load cell at the bottom of the loading device and generates the test bearing's loading up to 841 PSI (58 bar) specific loading by pushing the test bearing carrier platform device against the rotating shaft. A flexible hose inside the loading device housing provides lubricant oil from the loading device housing to the test bearing. An oil gallery allows for individual oil supply to the support bearings, the test bearing as well as to the planetary gear. Oil flows are measured by Coriolis-type flow meters. The complete train is mounted to a span baseplate levitated by means of air pillows, thus isolating the test-rig from the surroundings. As in most test rigs, oil flows, oil supply pressures as well as bearing pad temperatures and shaft vibration are monitored.

TESTS

In order to ensure that no oil channels inside the pad are obstructed, flow measurements of the cooling oil channels have been performed. For that, the leading-edge groove of the pad has been closed with the help of a piece of a tube with the corresponding pad diameter. Some rubber between pad and tube was used to seal the arrangement. An adapter screwed to the back of the pad was connected to the oil supply of the test-rig. With that test-set up, it was checked that the oil passages are free of any print powder left over and simultaneously the oil flow through the channels with different oil supply pressures could be determined.

The three-dimensional channels inside the AM pad complicate the installation of additional thermocouples in circumferential and axial direction. Therefore, the use of thermocouples was limited to the already foreseen standard thermocouple inserts of the pads. Although it does seem to be different, the final sensor locations of both pads, the AM one and the baseline one, are fully identical in terms of axial, radial and circumferential position. Figure 10 shows the instrumentation of the load carrying pads with thermocouples. The drillings of the test bearing's DE-side are equipped with thermocouples TP1 and TP3.

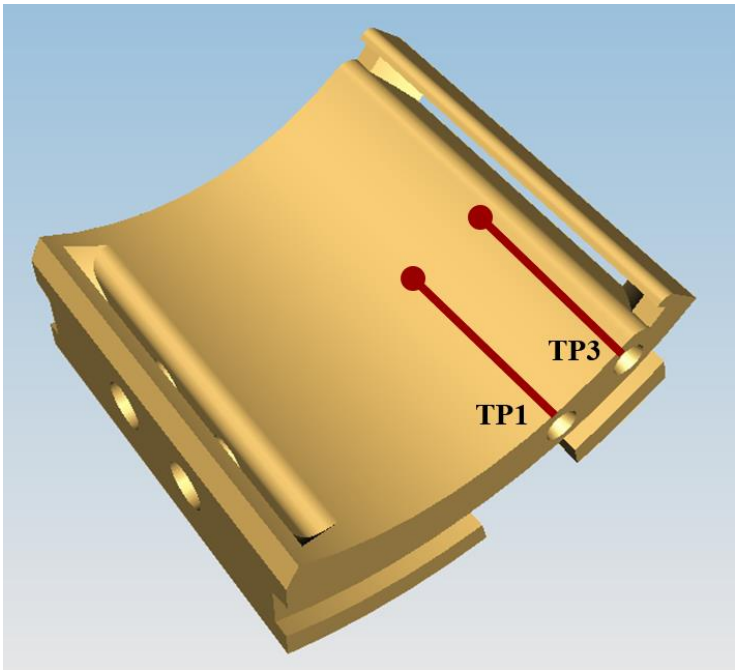

Figure 10. Instrumentation of Load Carrying Pads with Thermocouples

For the bearing tests, the oil flow to the test bearing as well as the specific bearing loading are kept constant. The rotational speed of the test rotor is varied in steps of 32.8 ft/s (10m/s) from 65.6 ft/s (20m/s) to 459.3 ft/s (140 m/s). Steady state conditions with the thermocouples are reached within less than 10 minutes. Then the test data are acquired and the next rotor speed is approached with repeating procedure. For the particular bearing testing, oil flows of 11.4 gal/min (43 ltr/min) and 15.3 gal/min (58 ltr/min) in combination with 5 specific bearing loadings from 72.5 psi (5 bar) to 362.6 psi (25 bar) are measured.

RESULTS

The positive influence of the internal cooling channels on the pads' maximum temperature is visualized in the following figures of this section. The upper part of Figure 11 shows the maximum measured pad temperature for both, the AM and the baseline pad versus circumferential speed for different specific bearing loads and an oil flow of 11.4 gal/min (43 ltr/min). The curves show the expected increase in temperature for increasing circumferential speed and increasing specific bearing load. The intersection of the temperature curves with the API 8th edition (2014) limit of 212 °F (100 °C) is shifted towards smaller circumferential speeds with increasing specific bearing load. Whereas this intersection for the baseline pad and the maximum tested specific bearing load of 362.6 psi (25 bar) is about 360.9 ft/s (110 m/s), the corresponding intersection of the AM pad is shifted by about 65.6 ft/s (20 m/s) to nearly 426.5 ft/s (130 m/s), showing the influence of the internal cooling. Analyzing the maximum pad temperature curves, a transition from laminar to turbulent flow regime in the region of 229.7 ft/s (70 m/s) to 328.1 ft/s (100 m/s) can be assumed. The maximum pad temperatures of the AM pad decline a bit and to increase again with increasing circumferential speed.

The corresponding differential temperatures between baseline and AM pad are shown in the lower part of Figure 11 with a measured maximum differential temperature of nearly 25 degrees F (14 degrees C) for 393.7 ft/s (120 m/s) circumferential speed and 362.6 psi (25 bar) specific bearing loading. The differential temperatures in the laminar to turbulent transition region do not show a clear trend. This changes with circumferential speeds above 328.1 ft/s (100 m/s). Here, the differential temperatures ascend with increasing circumferential speed as well as with increasing specific bearing load as expected. The lubricant is supplied to the inlet groove at the pad's leading edge and the cooling channels via the same supply openings so that both pad internal systems are coupled. With increasing circumferential speed and specific bearing load, the hydrodynamic pressure on the pads increases and raises the resistance for the supply lubricant leaving the inlet groove at the pad's leading edge. Hence, the lubricant will leave the pad by the cooling channels with a smaller flow resistance, thus increasing the "cooling oil flow" and further improving the cooling mechanism.

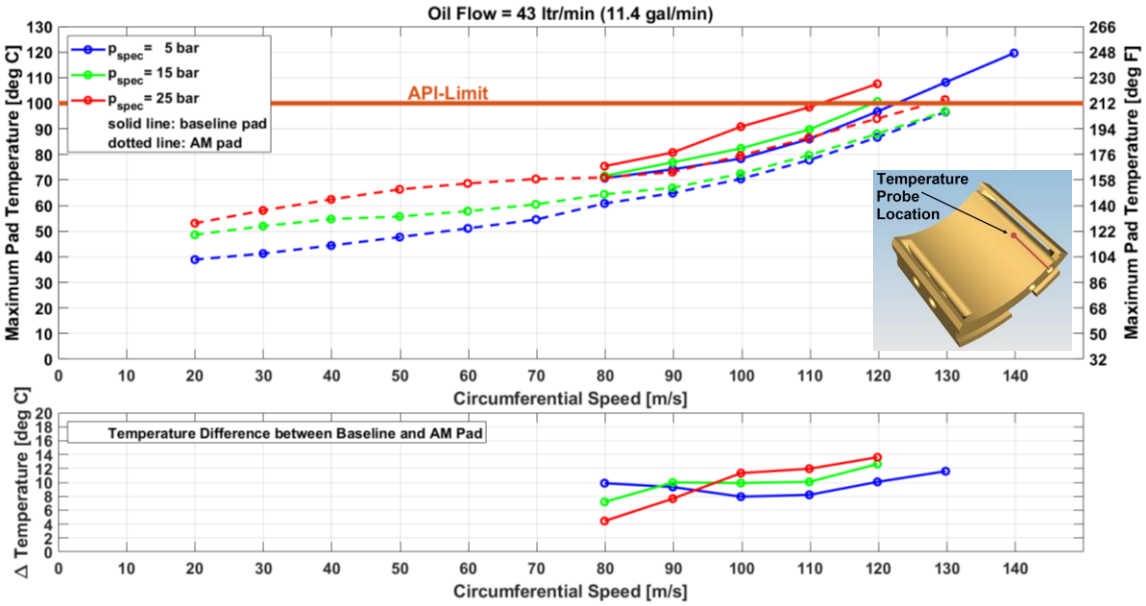

Figure 11. Test Results: Maximum Pad Temperature for Variation of Circumferential Speed and Specific Bearing Loading for Oil Flow of 11.4 gal/min (43 ltr/min)

Figure 12 below shows the identical test data representation as Figure 11 but for an oil flow of 15.3 gal/min (58 ltr/min). Maximum measured pad temperatures show the identical ascending trend for increasing circumferential speed and specific bearing loading as with a smaller oil flow. Again, for the maximum tested specific bearing loading of 362.6 psi (25 bar) the intersection with the API limit is shifted by approximately 65.6 ft/s (20 m/s) from 393.7 ft/s (120 m/s) to 459.3 ft/s (140 m/s). Whereas the maximum pad temperatures also show the transition from laminar to turbulent flow regime in the region of 229.7 ft/s (70 m/s) to 328.1 ft/s (100 m/s), the differential temperatures in the lower part of the figure do show a clear rise for 217.6 psi (15 bar) and 362.6 psi (25 bar) specific bearing loading. Beyond 328.1 ft/s (100 m/s), the differential temperatures for 72.5 psi (5 bar) and 217.6 psi (15 bar) specific bearing loading decline while the differential temperatures for 362.6 psi (25 bar) specific bearing loading increase up to a maximum value of about 25 degrees F (14 degrees C). For low specific bearing loads and increasing circumferential speeds it seems that the lubricant supply pressure is higher than the hydrodynamic pressure, thus forcing the lubricant to leave the pad via the inlet groove at the pad's leading edge and not by the cooling channels.

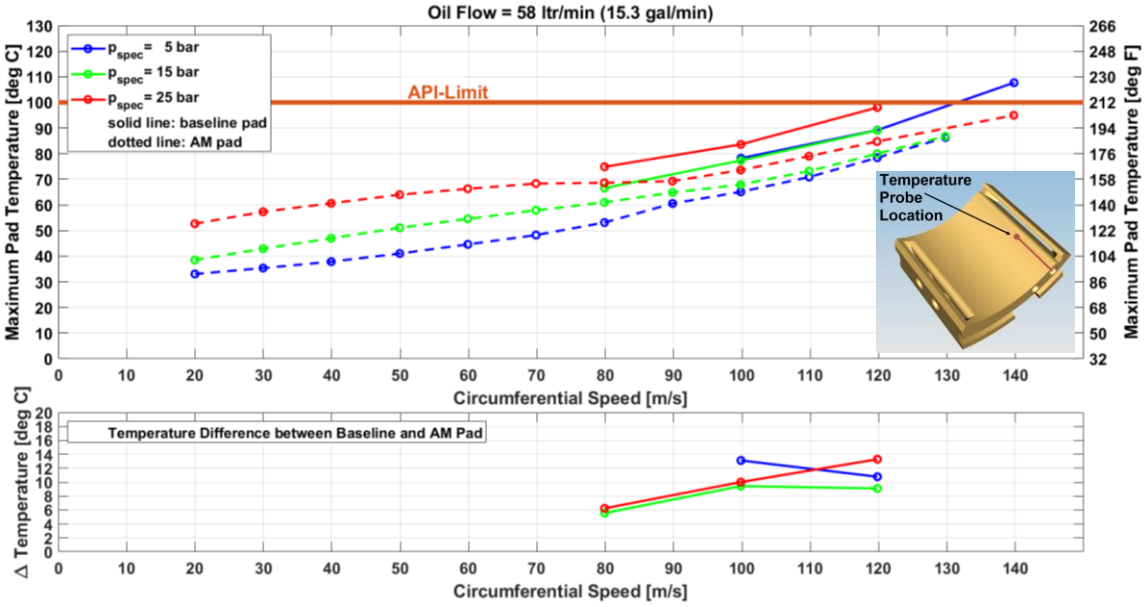

Figure 12. Test Results: Maximum Pad Temperature for Variation of Circumferential Speed and Specific Bearing Loading for Oil Flow of 15.3 gal/min (58 ltr/min)

For all tested oil flows and specific bearing loadings, the maximum pad temperatures converge for increasing circumferential speed; indicating that the specific bearing load is of secondary importance for highest circumferential speeds. This behaviour becomes even more evident with the depictions of Figure 13 and Figure 14 showing the maximum pad temperatures as isothermal curves versus specific bearing loading and circumferential speed for different oil flows. In both figures, the isothermal curves become more and more vertical with increasing circumferential speed. For small circumferential speeds up to approximately 328.1 ft/s (100 m/s), the isothermal curves are more diagonal, showing the larger influence of specific bearing loading on pad temperature than of circumferential speed. Passing this threshold value to higher circumferential speeds, this behaviour turns and the circumferential speed becomes the primary influence on pad temperature.

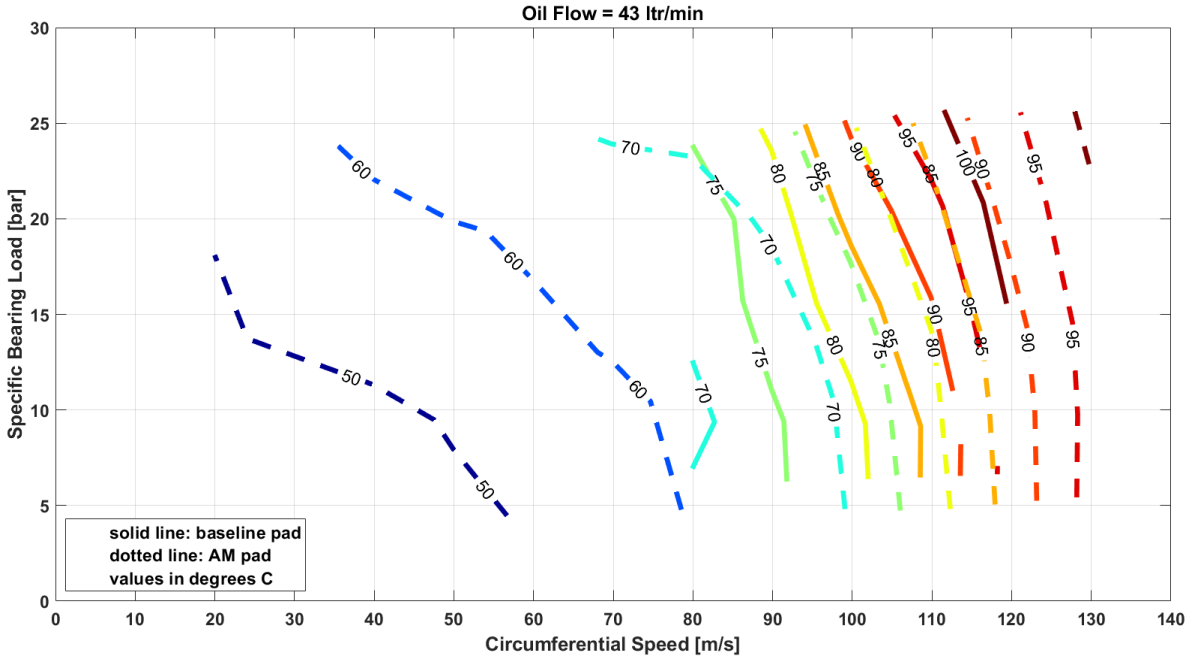

Figure 13. Isothermal Curves of Maximum Measured Pad Temperature for Variation of Circumferential Speed and Specific Bearing Loading for Oil Flow of 11.4 gal/min (43 ltr/min)

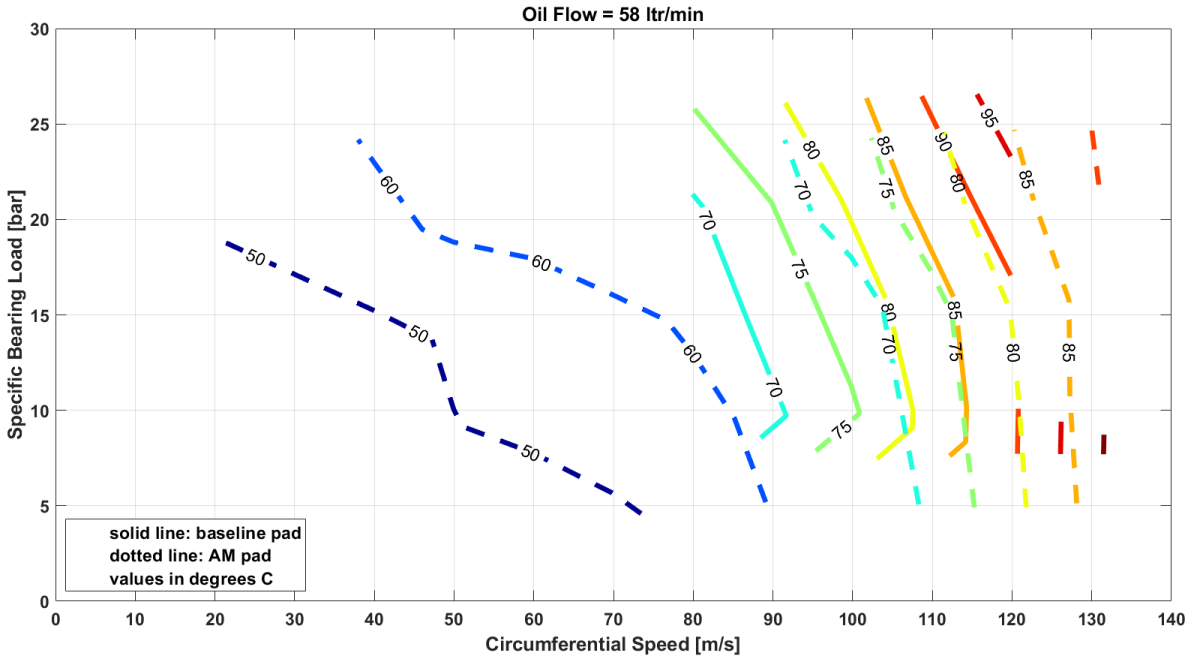

Figure 14. Isothermal Curves of Maximum Measured Pad Temperature for Variation of Circumferential Speed and Specific Bearing Loading for Oil Flow of 15.3 gal/min (58 ltr/min)

A direct comparison between the two different oil flows for the AM pad is shown in Figure 15. Increasing the oil flow from 11.4 gal/min (43 ltr/min) by 4 gal/min (15 ltr/min) to 15.3 gal/min (58 ltr/min) results in a 18 degrees F (10 degrees C) temperature difference for the maximum pad temperature or, expressed in circumferential speed, in an isothermal curve shift of 32.6 fts (10 m/s) towards higher circumferential speeds.

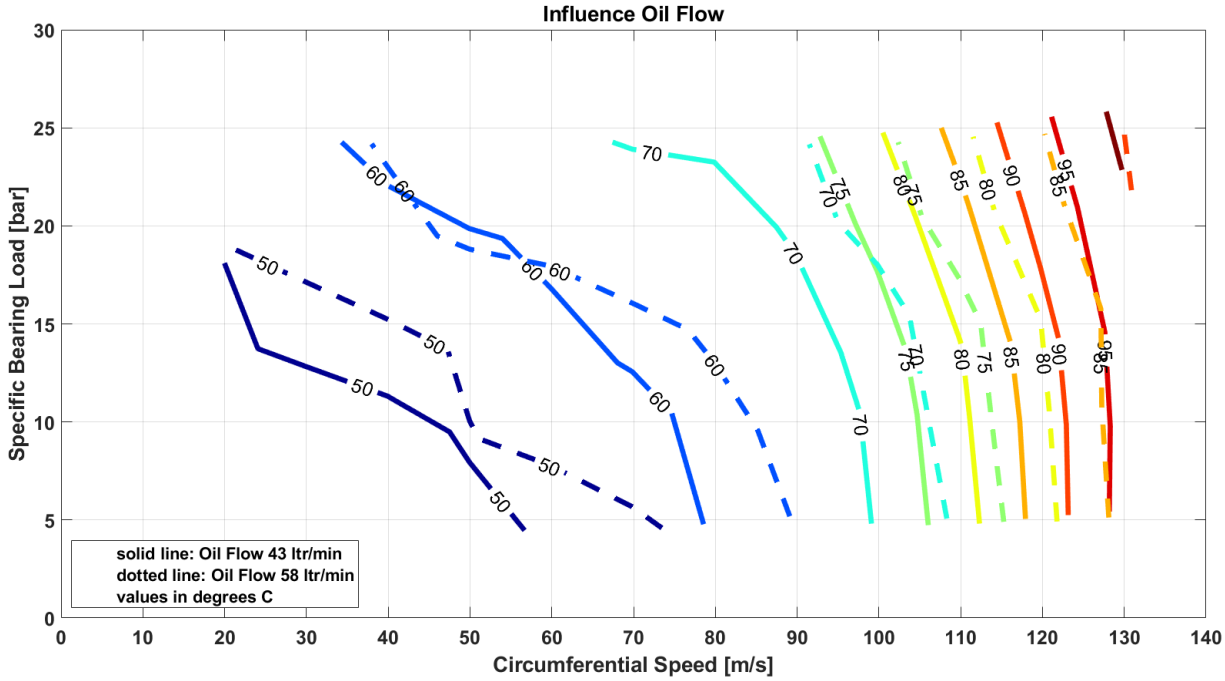

Figure 15. Isothermal Curves of Maximum Measured Pad Temperature for Different Oil Flows of the AM Pad

Beside the maximum pad temperature, the temperature gradient in the circumferential direction is of interest. Figure 16 below shows the pad temperatures at positions TP1 and TP3 at the axial centreline of the pads for different specific bearing loadings and circumferential speeds with an oil flow of 11.4 gal/min (43 ltr/min). With small specific bearing loadings, the load direction seems to be shifted a little bit to the upstream pad where the temperatures are higher than with the downstream pad. With increasing specific bearing load and circumferential speed the pads seem to settle and the downstream pads show higher temperatures than the upstream pads.

For the specific bearing loads of 217.6 psi (15 bar) and 362.6 psi (25 bar) the baseline pad's temperatures show an interesting trend. The temperatures TP3 of pad 1 and TP1 of pad 2 are nearly on the same level, showing that a certain hot-oil-carry-over from pad 1 to pad 2 takes place especially for high circumferential speeds. In opposition to that, the AM pad's temperatures do show a significant difference. The temperatures at TP1 of pad 2 are always less than TP3 of pad 1, indicating an effective hot-oil-carry-over prevention from pad 1 to pad 2. In fact, the AM pad's temperature gradients of pad 1 and pad 2 are about the same.

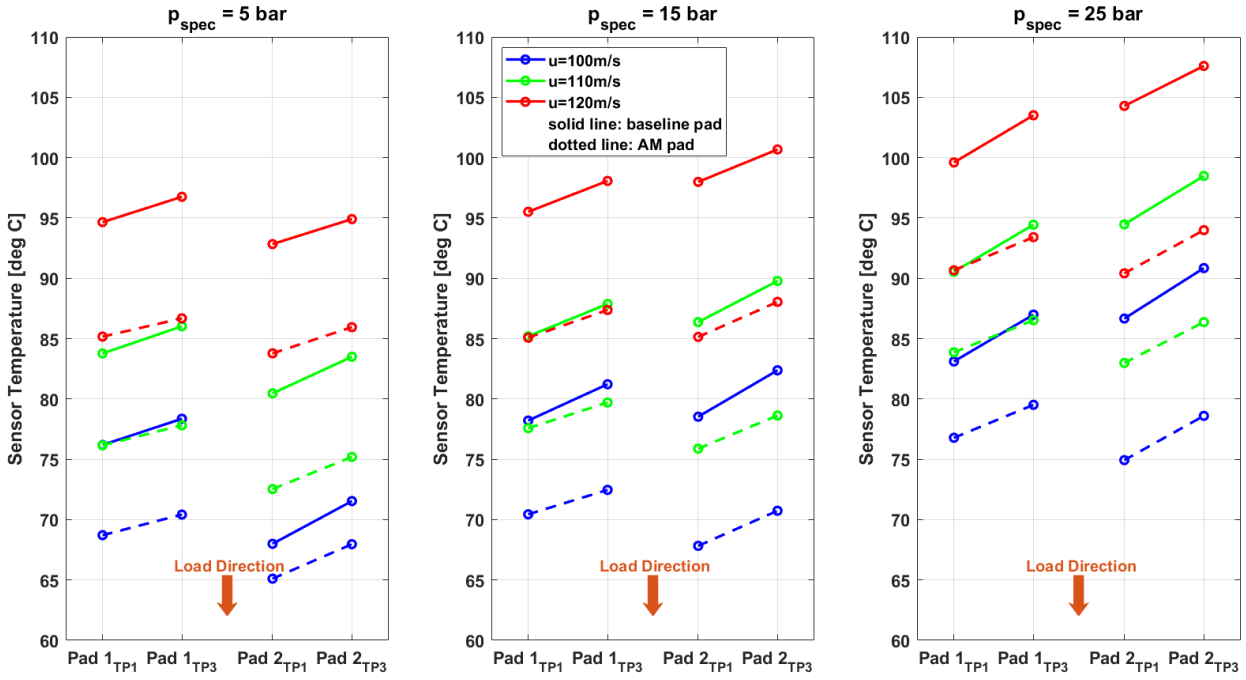

Figure 16. Measured Data: Temperature Gradients on Pad's Centreline for Different Specific Bearing Loadings and Circumferential Speeds with an Oil Flow of 11.4 gal/min (43 ltr/min)

The power losses of the tested configurations are shown in Figure 17 for different oil flows and specific bearing loadings. Power losses ascend with increasing circumferential speed. By increasing the oil flow from 11.4 gal/min (43 ltr/min) to 15.3 gal/min (58 ltr/min), the power loss increases by about 13.3 hp (10 kW). In the region of 229.7 ft/s (70 m/s) to 328.1 ft/s (100 m/s) the gradients of the power loss curves ascend, thus indicating a transition from laminar to turbulent flow regime. However, no distinct difference in power loss between the additive manufactured and the baseline pad is detectable.

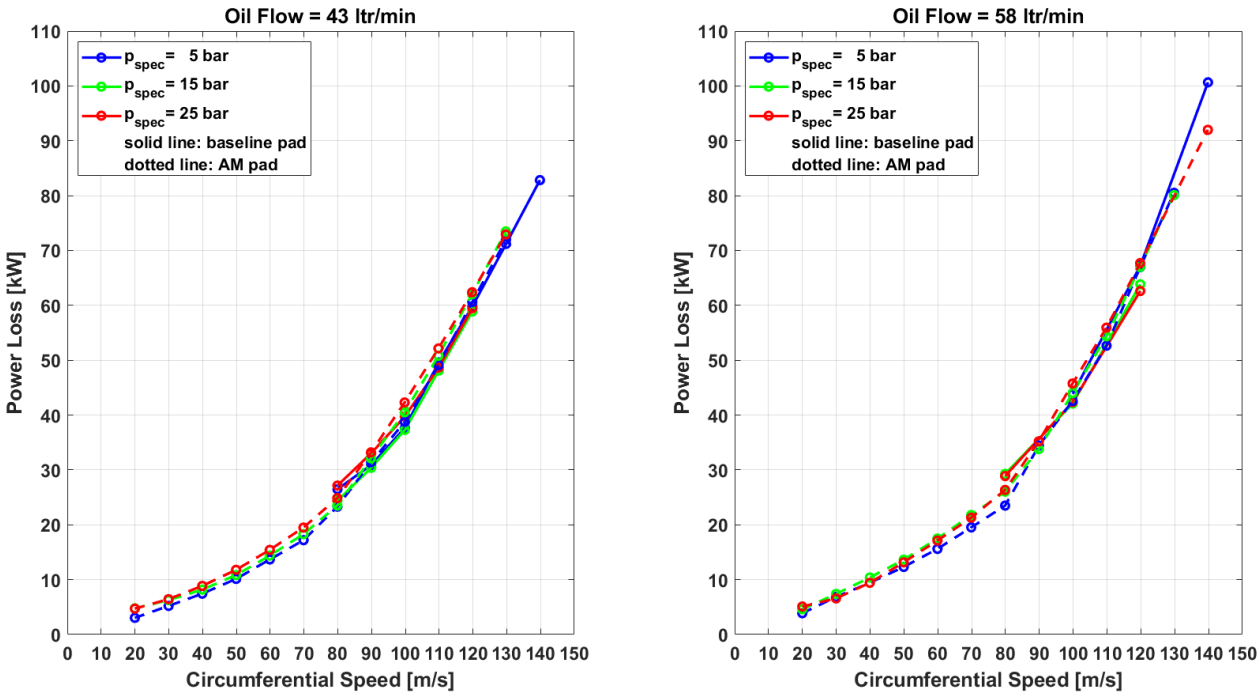

Figure 17. Measured Power Loss for Different Specific Bearing Loadings and Circumferential Speeds

CONCLUSION

A new concept to improve the performance of a hydrodynamic tilting pad bearing was presented. Additive manufacturing (AM) was used to produce tilting pad bearings with internal cooling channels. Arc spraying was used to coat the pads' sliding surface with Babbitt. Intensive bearing testing has been conducted for two bearings where only the baseline load carrying pads were replaced with the AM pads. Comparisons with baseline pads allowed for assessing the amount of cooling. Differences in maximum pad temperatures of up to 25 degrees F (14 degrees C) were measured, thus allowing for shifting the application range of the additive manufactured pads by 65.6 ft/s (20 m/s) towards higher circumferential speeds while still meeting API 617 8th Edition bearing temperature limits.

The technology was originally designed for high-speed and high-load gear-type compressor applications but it is also applicable to high-speed and low-load single-shaft compressor applications. Optimization of the internal cooling by use of Computational Fluid Dynamics (CFD) together with optimization strategies will further increase the AM pad's application range. Pressure and temperature transducers in the cooling cavities during testing will help to adjust CFD models and improve prediction accuracy.

Matching the test results with the results of a hydrodynamic bearing calculation code is a logical next step as all currently available calculation codes do not comprise calculation models for pad's internal cooling.

REFERENCES

API 617, 2014, "Axial and Centrifugal Compressors and Expander-Compressors", Eight Edition, American Petroleum Institute, Washington, D.C., USA

Becker, B., 2000, "Kühlbares Lager", Patent EP 1 002 965 A1, European Patent Office

Brockwell, K., Dmochowski, W., DeCamillo, S., Mikula, A., 1992, "Performance evaluation of the LEG tilting pad journal bearing ", Kingsbury Inc, USA

Hirotoshi, A., 2015, „Kippsegmentradiallager", Patent DE11 2016 000 505 T5

Livermore-Hardy, R., Blair, B., 2014, "Trailing Edge Cooled Bearing", Patent WO 2014/160493 A1, International Application published under the patent cooperation treaty

Minegishi, A., Taketomi, T., 2014, "Tilting Pad Bearing and Turbo Compressor", Patent EP3029343A1, European Patent Office

Nicholas, J.C., 2003, "Tilting Pad Journal Bearings with Spray-Bar Blockers and By-Pass Cooling for High Speed, High Load Applications," Proceedings of the Thirty-Second Turbomachinery Symposium

Nicholas, J.C., Shoup, T., Fiegl, A., Rockefeller, D., Ronan, J., 2014, "Reverse Bypass Cooling for Tilting Pad Journal and Tilting Pad Thrust Bearings", Patent WO2016/025508A1, International Application published under the patent cooperation treaty

Sato, M., Suzuki, K., Hemmi, M., 2016, "Tilting Pad bearing", US Patent US 2016/0169275

Takeshi, M., Makoto, H., Tetsuya, A., Hideto, N., 2009, "Tilting Pad Type Journal Bearing", Patent 2009063015 A

ACKNOWLEDGEMENTS

The contributions of Judith van Bevern-Janza and of the R&D Test Field crew to this project are highly appreciated.